

Looking for non-Gaussianity in the COBE-DMR data with spherical wavelets

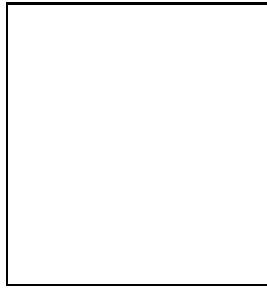
R.B.BARREIRO¹, M.P.HOBSON¹, A.N.LASENBY¹, A.J.BANDAY², K.M. GÓRSKI³
and G. HINSHAW⁴

¹ *Astrophysics Group, Cavendish Laboratory, Madingley Road, Cambridge CB3 0HE, UK*

² *Max-Planck Institut fuer Astrophysik (MPA), Karl-Schwarzschild Str.1, D-85740, Garching, Germany*

³ *European Southern Observatory (ESO), Karl-Schwarzschild Str.2, D-85740, Garching, Germany*

⁴ *NASA/GSFC, Greenbelt, MD 20771, USA*



We present an analysis of the Gaussianity of the 4-year COBE-DMR data (in HEALPix pixelisation) based on spherical wavelets. The skewness, kurtosis and scale-scale correlation spectra are computed from the detail wavelet coefficients at each scale. The sensitivity of the method to the orientation of the data is also taken into account. We find a single detection of non-Gaussianity at the $> 99\%$ confidence level in one of our statistics. We use Monte-Carlo simulations to assess the statistical significance of this detection and find that the probability of obtaining such a detection by chance for an underlying Gaussian field is as high as 0.69. Therefore, our analysis does not show evidence of non-Gaussianity in the COBE-DMR data.

1 Introduction

Testing the Gaussianity of the cosmic microwave background (CMB) fluctuations has become of great interest since it would make it possible to distinguish between competing theories of structure formation in the early Universe such as inflation and topological defects. With this aim, a large number of techniques have already been proposed, many of them being applied to the 4-year COBE-DMR data (see e.g. Barreiro 2000). Although most of these analyses did not find evidence for non-Gaussianity, methods based on bispectrum analyses (Ferreira et al. 1998, Magueijo 1999; see also Zaroubi et al. 1999) and on statistics of wavelet coefficients (Pando et al. 1998) have yielded detection of non-Gaussianity in the COBE-DMR data. In particular, Pando et al. have found a significant non-Gaussian signal at the 99% confidence level on computing the scale-scale correlation of the wavelet coefficients. This analysis has recently been revised by Mukherjee et al. (2000) (hereinafter MHL) who take into account that the results depend critically on the orientation of the signal and that a large number of the computed statistics do

not show deviation from the Gaussian case. According to MHL, Gaussianity can be ruled out only at the 41% confidence level in the DSMB data and at the 72% level in the 53+90 GHz coadded data. The above wavelet analyses have been performed applying planar wavelets to Face 0 and Face 5 of the COBE-DMR QuadCube pixelisation. Therefore only one-third of the available data is being considered and, at the same time, undesirable projection effects may be present. In this work, we have performed a similar analysis to those of Pando et al and MHL, but applying orthogonal spherical Haar wavelets (SHW) (see Sweldens 1995 and references therein) to the COBE data in HEALPix pixelisation (Górski et al 1999) with the customised Galactic cut (Banday et al. 1997). On the one hand, this hierarchical pixelisation scheme is particularly well-suited to the application of such a wavelet decomposition. On the other hand, SHW are more appropriate to study data over a large region of the sky and also allow an easy identification of those coefficients affected by the Galaxy. Therefore *all* data lying outside the Galactic cut is used in the analysis, i.e., approximately two-thirds of the total number of COBE-DMR pixels.

As an illustration, we present our results for three different orientations of the data to account for the sensitivity of these estimators to the orientation of the input signal.

2 The wavelet analysis

We have used the coadded 53+90 GHz COBE-DMR map (each weighted according to the inverse of its noise variance) in HEALPix pixelisation (see Banday et al. 2000 for the map-making) with the customised Galactic cut. HEALPix is an equal area, iso-latitude and hierarchical pixelisation of the sphere. The resolution level of the grid can be expressed by a parameter j (or equivalently N_{side} with $N_{side} = 2^{j-1}$). The lowest resolution ($j = 1$) comprises twelve pixels in three rings around the poles and equator. To move to a higher resolution level, each pixel at resolution j is divided into four pixels at resolution $j + 1$. Therefore the total number of pixels at a given resolution j is $n_j = 12 \times 4^{j-1}$. The COBE-DMR maps correspond to a resolution $J = 7$.

Orthogonal SHW are not translations and dilations of a given function and so can be adapted to more general spaces than R^n (Sweldens 1995). In addition, they still enjoy the usual properties of planar wavelets such as a good frequency-space localisation and a fast transform algorithm. The temperature field can be decomposed in terms of the SHW basis functions as

$$\frac{\Delta T}{T}(x_i) = \sum_{l=0}^{n_{j_0}-1} \lambda_{j_0,l} \varphi_{j_0,l}(x_i) + \sum_{j=j_0}^{J-1} \sum_{m=1}^3 \sum_{l=0}^{n_j-1} \gamma_{m,j,l} \psi_{m,j,l}(x_i) \quad (1)$$

where $\lambda_{j_0,l}$ and $\gamma_{j,m,l}$ are the approximation and detail wavelet coefficients respectively. The first term in the previous equation corresponds to a coarser resolution image of the original map whereas the detail coefficients encode the difference between both maps. The index j runs from the lowest resolution considered j_0 to $J - 1$. Finally, the index m corresponds to the three different wavelet functions at each scale needed to have a wavelet basis. In order to get the wavelet coefficients, one starts identifying the pixels at the map resolution J with the approximation coefficients $\lambda_{J,l}$. Then each wavelet coefficient at resolution $J - 1$ is obtained as a linear combination of the four corresponding coefficients at resolution J . In this way, the approximation coefficients $\lambda_{J-1,l}$ and three sets of detail coefficients $\gamma_{1,J-1,l}$, $\gamma_{2,J-1,l}$ and $\gamma_{3,J-1,l}$ at scale $J - 1$ are obtained. The same process is performed again but starting with the $\lambda_{J-1,l}$ coefficients as our initial map to obtain the wavelet coefficients at $J - 2$ and then the process is repeated down to the lowest resolution considered j_0 (for a more detailed description see Barreiro et al. 2000, Tenorio et al. 1999).

In our wavelet analysis, we obtain estimators for the skewness $\hat{S}(j, m)$, (excess) kurtosis $\hat{K}(j, m)$ and scale-scale correlation $\hat{C}^2(j, m)$ (as defined in Barreiro et al. 2000) of each type m of detail wavelet coefficients at each scale j . In order to perform our non-Gaussianity test, we

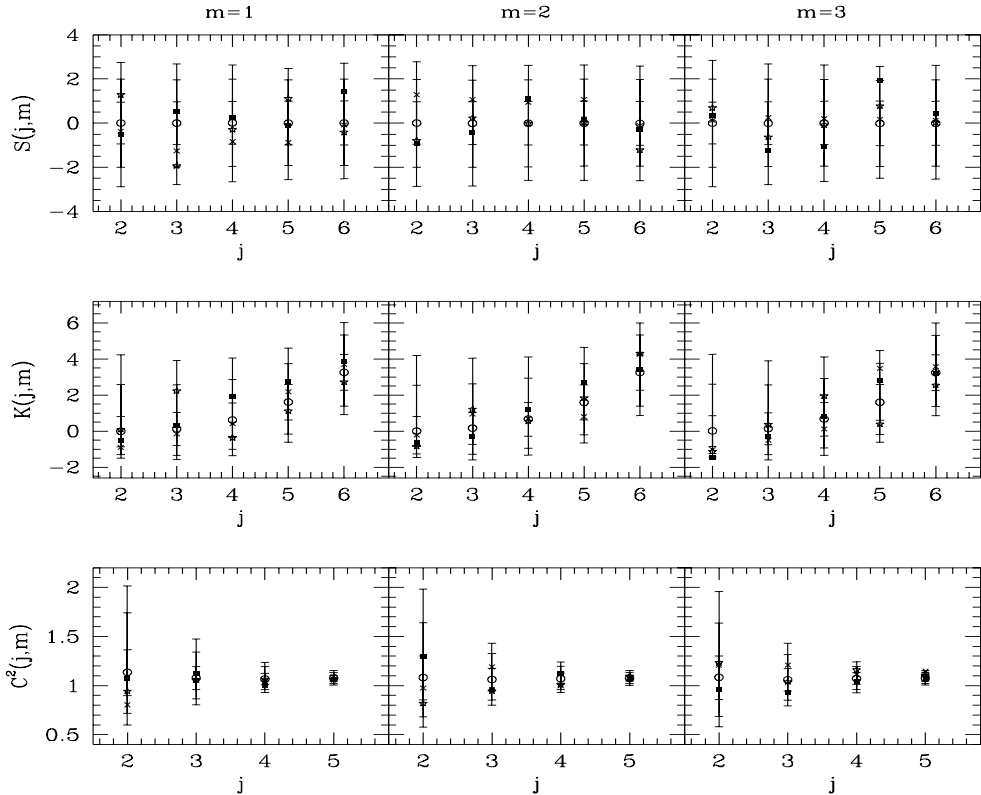


Figure 1: The skewness, kurtosis and scale-scale correlation spectra for the 53+90 GHz COBE map are plotted for each type of detail coefficients $m = 1, 2, 3$ (first, second and third column respectively). See text for details.

first obtain the previous quantities for the coadded 53+90 GHz COBE-DMR map, discarding those wavelet coefficients coming from pixels inside the Galactic cut. Then the same estimators are obtained for a large number (10000) of CMB all-sky simulated maps, that take into account the characteristics of the COBE-DMR data. In this way, we can obtain approximate probability distributions for the $\hat{S}(j, m)$, $\hat{K}(j, m)$ and $\hat{C}^2(j, m)$ statistics for a CMB signal derived from the chosen model. In particular, the CMB simulations are drawn from a inflationary/ Λ CDM model with parameters $\Omega_m = 1$, $\Omega_\Lambda = 0$, $h = 0.5$, $n = 1$ and $Q_{rms-ps} = 18\mu K$ but we do not expect our results to vary significantly with a different choice of parameters (see MHL). By comparing these distributions with the values computed from the COBE-DMR data, we can obtain the probability that our data are derived from a Gaussian distribution characterised by the chosen power spectrum. In addition, since the wavelet decomposition is sensitive to the orientation of the data, we perform the previous test for three different orientations of the sky. Therefore we compute a total of $42 \times 3 = 126$ statistics for each map.

3 Results

The computed $\hat{S}(j, m)$, $\hat{K}(j, m)$ and $\hat{C}^2(j, m)$ spectra are plotted in Fig. 1 for three different orientations. We rotate the 53+90 COBE-DMR map around an axis passing through the North and South Galactic poles. A rotation of 90 degrees around this direction simply shifts the twelve base-pixels of the HEALPix pixelisation into each other and therefore gives rise to the same results as the original orientation. We show the results computed from the COBE-DMR data for a rotation of 0 (orientation A, solid squares), 30 (orientation B, crosses) and 60 (orientation C, stars) degrees with respect to the original orientation of the map. The open circle and error

bars correspond to the average value and the 68, 95 and 99% confidence levels of the distribution obtained from the 10000 CDM realisations for orientation A. We do not plot the corresponding error bars for orientations B and C in Fig. 1 for the sake of clarity and because the conclusions derived from the plot remain unchanged. For convenience, the skewness and kurtosis spectra have been normalised at each value of (j, m) such that the variance of the distribution obtained from the 10000 CDM realisations is equal to unity. We can see in Fig. 1 that the COBE-DMR values of the $\hat{S}(j, m)$ and $\hat{C}^2(j, m)$ spectra for orientations A,B and C are consistent with being derived from a parent Gaussian distribution. However, we find a detection of non-Gaussianity in the $\hat{K}(j, m)$ spectra at $j = 2$ and $m = 3$ at the $> 99\%$ confidence level for orientation A, the rest of the values lying within their respective Gaussian probability distributions.

In order to assess the statistical significance of this detection and since most of our statistics show no evidence of non-Gaussianity, we have used Monte-Carlo simulations to estimate the probability of having at least one detection of non-Gaussianity at the $\geq 99\%$ confidence level out of our 126 statistics for an underlying Gaussian field. We find that this occurs in 69% of the cases and therefore this analysis does not provide strong evidence of non-Gaussianity in the COBE-DMR data. This is in agreement with the results obtained by MHL.

We have also checked that the general conclusions regarding non-Gaussianity are not affected, at least in our case, by the choice of a different set of orientations (see Barreiro et al. 2000).

4 Conclusions

We have investigated the Gaussianity of the 4-year COBE data (in HEALPix pixelisation) with an analysis based on SHW. We have taken into account the sensitivity of our method with respect to the orientation of the input signal, presenting the results for three different orientations.

We have found a single detection of non-Gaussianity at the $> 99\%$ confidence level out of our 126 computed statistics, corresponding to the value of the kurtosis at $j = 2, m = 3$ for one of the chosen orientations. Using Monte-Carlo simulations we estimate that the probability of having such a detection in one of our statistics is as high as 0.69 for the case of an underlying Gaussian field. Therefore, we conclude that an analysis based on SHW of the 4-year COBE-DMR data show no evidence of non-Gaussianity in the CMB.

Acknowledgements

RBB thanks Luis Tenorio for helpful comments about spherical wavelets. We thank all the people involved in producing the HEALPix package, which has been extensively used along this work. RBB acknowledges financial support from the PPARC in the form of a research grant.

1. Banday A.J. et al., 2000, in preparation
2. Banday A.J. et al., 1997, *ApJ*, 475, 393
3. Banday A.J., Zaroubi S., Górski K.M., 2000, *ApJ*, in press (astro-ph/9908070)
4. Barreiro R.B., 2000, *New Astr.Rev.*, in press (astro-ph/9907094)
5. Barreiro R.B. et al., 2000, submitted (astro-ph/0004202)
6. Ferreira P., Magueijo J., Górski K.M., 1998, *ApJ*, 503, L1
7. Górski K.M., Hivon E., Wandelt B.D., 1999, in ‘Evolution of Large-Scale Structure: from Recombination to Garching’, p.37, PrintPartners Ipskamp; <http://www.tac.dk/~healpix>
8. Magueijo J., 2000, *ApJ*, 528, L57 (see also Magueijo J., 2000, *ApJ*, 532, L157)
9. Mukherjee P., Hobson M.P., Lasenby A.N., 2000, *MNRAS*, in press (MHL)
10. Pando J., Valls-Gabaud D., Fang L.-Z., 1998, *Phys.Rev.Lett.*, 81, 4568
11. Sweldens W., 1995, Technical Report, University of South Carolina
12. Tenorio L., Jaffe A.H., Hanany S., Lineweaver C.H., 1999, *MNRAS*, 310, 823